

Direct Torque Control of Induction Motor Fed by Three-level Inverter Using Fuzzy Logic

BERRABAH Fouad*, CHEBABHI Ali***, ZEGHLACHE Samir*, SAAD Salah**

*Department of Electrical Engineering, University of M'sila, Algeria, BP-166 University of M'Sila
28000 (fouadberrabah1@gmail.com)

** Laboratory Systèmes Electromécaniques (LSELM), University of Annaba, Algeria

***ICEPS Laboratory (Intelligent Control & Electrical Power Systems). Djillali Liabes University
of Sidi Bel-Abbes Algeria

*** Faculty of Science and Technology, University of Bordj Bou Arreridj, Algeria

Abstract

The present paper describes the direct torque sensor less speed control of induction motor fed by three-level voltage source inverter. Inverter switches control is based on fuzzy logic control. Compared to conventional direct torque control (DTC), hysteresis controllers, flux position and voltage vector selection table are replaced by fuzzy logic blocks to realize a DTC-fuzzy control. The obtained results have showed high speed performance, reduced torque and flux fluctuations when the proposed DTC-fuzzy strategy is used for the control of three-level voltage source inverter associated with induction machine.

Keywords

DTC, Fuzzy logic, DTC- FLC, Three-level NPC Inverter.

1. Introduction

Asynchronous motors particularly induction motors are widely used in variable speed drive systems due to their low cost and construction simplicity. The direct torque control technique

(DTC) introduced in 1985 is an attractive approach due to its effectiveness and implementation simplicity as demonstrated by several studies [1-6]. Therefore, this technique enables the control variables computation (stator flux and electromagnetic torque) from stator current measurements without using mechanical sensor.

In DTC structure, the induction motor fed by voltage source inverter is a hybrid dynamic system in which the continuous part is the induction machine and the discrete part is the voltage source inverter. In this paper, the application of DTC-fuzzy strategy concept is extended to a three-level voltage source inverter feeding asynchronous motor. This extension concerns the generation of voltage vector applied to the machine according to the number of voltage levels generated by the three-level inverter [3, 5, 7, 8]. This new direct torque control approach improves controller switching strategy of flux and torque of induction machine fed by a three-level NPC inverter.

Recently, optimization of DTC algorithms based on two-level inverter was studied in several papers [5, 7]. However, the main motivation of the present paper is to improve ac motors performances using a control approach based on so-called DTC-fuzzy control. Hysteresis blocks of torque and flux as well as the switching table of the conventional system are replaced by a set of fuzzy system. Three-level voltage source inverter (VSI) switching laws are determined by linguistic rules of fuzzy decision table and the speed is controlled by a conventional PI controller. This control structure reduces torque and flux fluctuations. In this paper, the DTC technique basic principle is explained and recalled [9-13], then, the model of three-level voltage inverter is presented. Finally, the DTC-fuzzy control technique is described, system performances are analyzed, and a conclusion is given.

The developed algorithm is validated by computer simulation tests using Matlab-Simulink environment. The obtained results have showed high speed performance, torque and flux reduced fluctuations when the proposed DTC-FLC strategy is employed for the control of three-level voltage source inverter associated with asynchronous machine.

2. Theoretical development of direct torque control

2.1 Electromagnetic torque control

Electromagnetic torque (C_{em}) is expressed in function of stator (ϕ_s) and rotor (ϕ_r) fluxes as follows [1]:

$$C_{em} = K \cdot \Im_m[\phi_s \cdot \phi_r] \quad (1)$$

K is a constant depending on machine parameters.

$$K = \frac{3}{2} \cdot P_n \cdot \frac{M_{sr}}{\sigma L_s L_r} \quad (2)$$

Stator and rotor fluxes can be expressed as follows:

$$\begin{cases} \phi_s = [\phi_s, \theta_s] = \phi_{s0} \cdot e^{j\theta_{s0}} \\ \phi_r = [\phi_r, \theta_r] = \phi_{r0} \cdot e^{j\theta_{r0}} \end{cases} \quad (3)$$

ϕ_{s0} and ϕ_{r0} are stator and rotor fluxes modules respectively at $t = 0$. θ_s and θ_r are stator and rotor

Substituting stator and rotor fluxes expressed in Eq.3 in the electromagnetic torque equation given in Eq.1.

Knowing that the control law desires to maintain the stator flux close to its reference value $\phi_{sréf}$, the following expression is obtained [5]:

$$C_{em} = K \cdot \phi_{sréf} \phi_{r0} \sin(\gamma_0) \quad (4)$$

$$\gamma_0 = \theta_{s0} - \theta_{r0} \quad (5)$$

When applying "active" voltage vector so that, the positions and rotor speeds and stator fluxes are modified as follows:

$$\phi_s = \phi_{sréf} \cdot e^{j(\theta_{s0} + \theta_{r0})} \quad (6)$$

Where:

$$\Delta\theta_s = (\omega_{s0} + \Delta\omega_s) \quad (7)$$

ω_{s0} = Synchronous speed

The expression above is the stator vector speed variation, similarly the rotor flux can be written as follows:

$$\phi_r = (\phi_{r0} + \Delta\phi_r) \cdot e^{j(\theta_{r0} + \Delta\theta_r)} \quad (8)$$

with: $\Delta\theta_r = \Delta\theta_s - \Delta\gamma$

If the evolution of the rotor flux is considered very slow compared to the stator flux, the implementation of active voltage vectors $\Delta\phi_r$ and $\Delta\theta_r$ are still zero, and thus:

$$\Delta\gamma = (\omega_{s0} + \Delta\omega_s) \tag{9}$$

The torque control depends directly on the stator flux vector rotation control. Fig.1, illustrates the evolution of the electromagnetic torque in the case of the application of two voltage vectors that are changing the stator flux in opposite direction of rotation. The trigonometric rotation direction is considered as the positive direction.

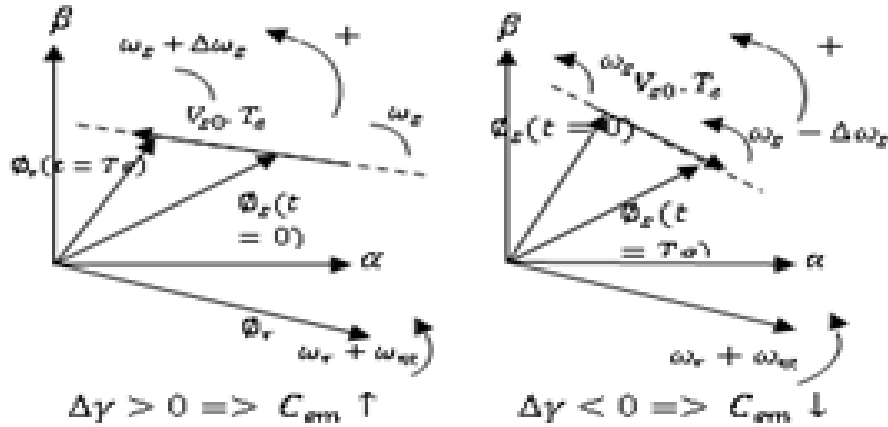


Figure 1. Electromagnetic torque evolution for rotational speed variation.

2.2 Stator flux vector control

The stator flux modulus evolution law is determined from the differential equation of the stator flux expressed in fixed frame (α, β) .

$$\frac{d}{dt} \phi_s = V_s - R_s i_s \tag{10}$$

V_s = Stator voltage

R_s = Rotor resistance

i_s = Stator current

In the interval $[0, T_s]$, the term $R_s \cdot i_s$ can be simplified and equation (10) can be written as follows [2].

$$\phi_s(T_e) \approx \phi_s(0) + V_s T_e \rightarrow V_s T_e \approx \Delta \phi_s \tag{11}$$

T_e = Sampling period

It should be noted that the extremity of the stator flux vector is moving along a straight line to that of collinear axis to the voltage vector imposed by the inverter to the machine Fig. 2 [1].

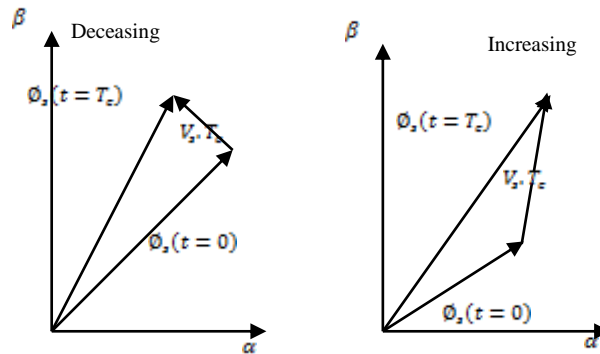


Figure 2. Statoric flux variation.

The stator flux vector displacement is achieved by successive application of voltage vectors fed by the inverter. Furthermore, according to the applied voltage vector, one can act on the value of the stator flux modulus as shown in Fig.2.

Thus, according to the choice of the stator voltage vector on successive intervals of the sampling period T_e duration, can be tacked at the extremity of the stator flux vector a trajectory almost circular and maintain the flux amplitude close to a constant reference value. This is illustrated by Fig.3 which corresponds to an example of asynchronous machine fed by two-level voltage source inverter. The stator flux is maintained in a hysteresis band centered on the reference flux [4].

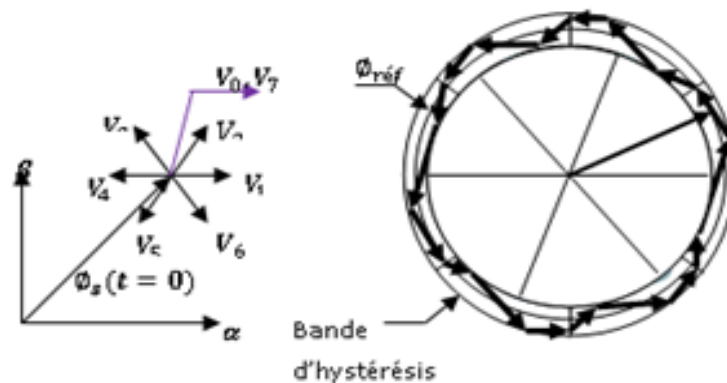


Figure 3. Statoric flux trajectory.

3. Three-level voltage inverter operation and modeling

The technological progress in induction machines variable speed control has advantaged the use of three-level inverters. As discussed previously, the increase in the number of levels proves to be a better solution for high power drives.

The inverter consists of switching cells usually transistors or GTO for high power. The association of asynchronous machine and three-level NPC voltage source inverter (VSI) controlled by DTC algorithms is presented and studied. The midpoint inverter is the most appropriate because the output voltages and output currents present less harmonic distortion than that obtained with a classical inverter [4].

The power circuit of three-level inverter called Neutral Point Clamped (NPC) is given in the Fig.4. It is a structure with three-level voltage. Each inverter leg consists of four switches; K_{n1} , K_{n2} , K_{n3} , and K_{n4} .

The mathematical model of this inverter is given by the following matrix:

$$\begin{bmatrix} V_A \\ V_B \\ V_C \end{bmatrix} = \frac{1}{3} \begin{bmatrix} 2 & -1 & -1 \\ -1 & 2 & -1 \\ -1 & -1 & 2 \end{bmatrix} \cdot \begin{bmatrix} S_{11}S_{12} - S_{13}S_{14} \\ S_{21}S_{22} - S_{23}S_{24} \\ S_{31}S_{32} - S_{33}S_{34} \end{bmatrix} U_c \quad (12)$$

Each inverter leg has three switching states as illustrated in Table I.

$V_A, V_B, \text{ and } V_C$: Phase-to neutral voltages

S_{ni} : The logical switching state

U_{dc} : dc voltage

Table 1. Three-level inverter switching states.

| Switches state | S_1 | S_2 | S_3 | S_4 | V_{KN} |
|----------------|-------|-------|-------|-------|------------|
| $S_n = 1 = P$ | 1 | 1 | 0 | 0 | U_{dc} |
| $S_n = 0 = O$ | 0 | 1 | 1 | 0 | $U_{dc}/2$ |
| $S_n = -1 = N$ | 0 | 0 | 1 | 1 | 0 |

Table 2. Voltage vectors associated to the switching states.

| Voltage vector | Symbol |
|----------------|--|
| ZVV | $(PPP); (OOO); (NNN)$ |
| MVV | $(PON); (OPN); (NPO); (NOP); (ONP); (PNO)$ |
| LVV | $(PNN); (PPN); (NPN); (NPP); (NNP); (PNP)$ |
| USVV | $(POO); (PPO); (OPO); (OPP); (OOP); (POP)$ |
| LSVV | $(ONN); (OON); (NON); (NOO); (NNO); (ONO)$ |

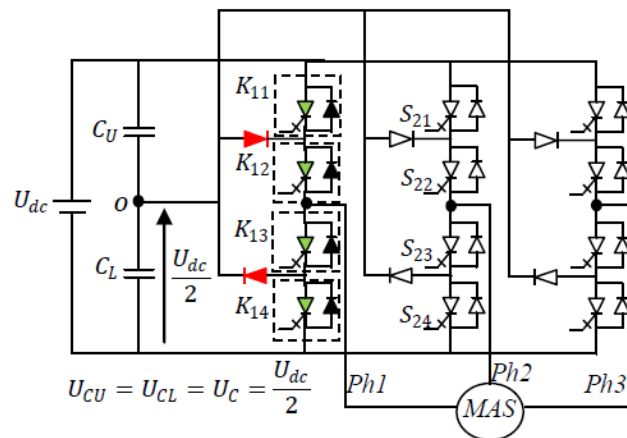


Figure 4. Three-level NPC voltage source inverter (VSI).

Table 2 shows 27 switching states of the inverter. According to these states 19 voltage vectors V_5 with different modulus are obtained [3-4].

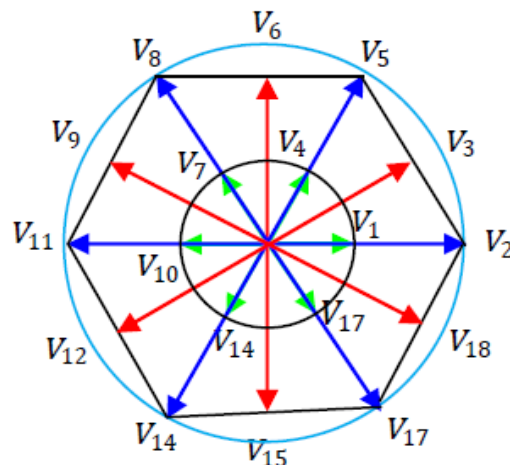


Figure 5. Output voltage vector representation.

Fig.5 shows that these voltage vectors are classified into four groups and according to their modulus it can be defined as follows:

- ZVV group, zero voltage vector V_0
- SVV group, small voltage vectors ($V_1, V_4, V_7, V_{10}, V_{13}, V_{16}$)
- MVV group, medium voltage vectors ($V_3, V_6, V_9, V_{12}, V_{15}, V_{18}$)
- LVV group, large voltage vectors ($V_2, V_5, V_8, V_{11}, V_{14}, V_{17}$)

Zero vector has three switching states, small vectors have two switching states (USVV, LSVV), medium and large vectors have only one switching state as example voltage vector V_2 corresponds to PNN state. Logical variables associated with the latter are [3]:

$$\begin{cases} S_{11} = 1, S_{12} = 1, S_{13} = 0, S_{14} = 0 \\ S_{21} = 0, S_{22} = 0, S_{23} = 1, S_{24} = 1 \\ S_{31} = 0, S_{32} = 0, S_{33} = 1, S_{34} = 1 \end{cases} \quad (13)$$

In terms of inverter control, this topology offers the following advantages:

- High number of degrees of freedom compared to two-level inverter,
- Reduced output current ripple,
- Remarkable property of interlocking hexagons, concept of two-level three-phase cell.

4. Direct torque control with fuzzy logic control (DTC-Fuzzy)

In the conventional direct torque control, the use of torque and flux errors allows to choose directly the switching state without distinguishing between a very large or relatively small error. Furthermore, the selected switching state for a large error that occurs during startup or during torque and flux set points change is the same as in normal operation. This obviously implies poor response.

System performance can be improved if the voltage vector is selected according to the value of torque and flux error as well as the flux position in the space of its evolution.

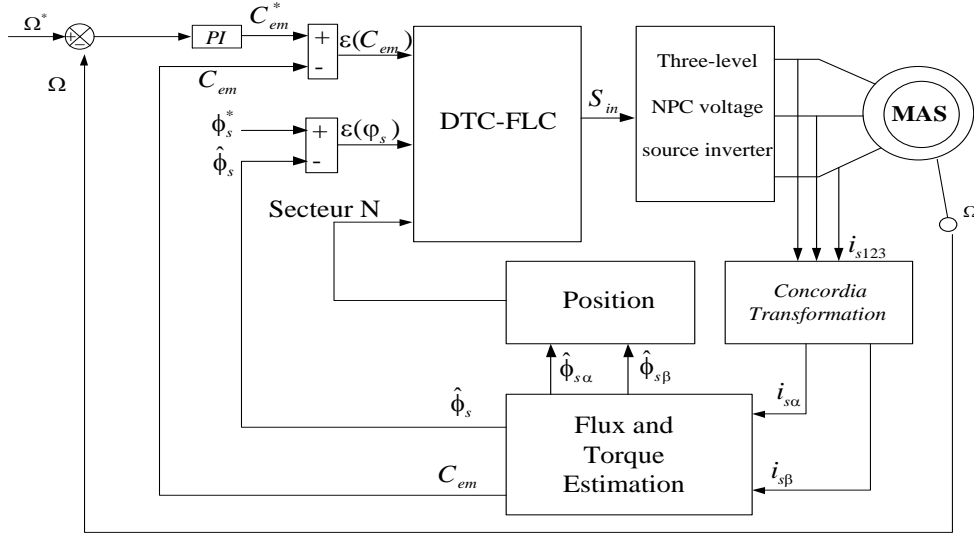


Figure 6. DTC-Fuzzy control scheme.

This error function is the difference between parameter computed from the information provided by the control and the equivalent parameter determined from measurements. The principle of fuzzy logic employing fuzzy concept can be applied to many problems when handling imprecise and indistinct parameters. It will be seen later, the advantage of this mode of analysis from the expertise rules defined by the inputs. The principle of DTC-FLC is illustrated in Fig.6.

A. Fuzzy logic control development

The speech universe of the first input variable ϵ_{ϕ} is divided into three fuzzy sets:

- Flux error is positive P
- Flux error is zero Z
- Flux error is negative N

The trapezoidal membership functions are chosen for the variables P, N and triangular for Z set Fig.7.

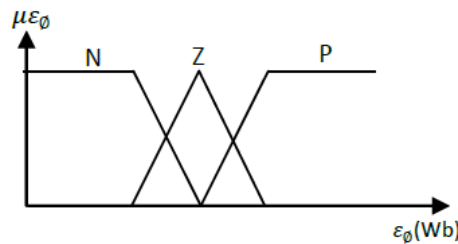


Figure 7. Membership function of flux error ϵ_{ϕ} .

The second input is the torque error ϵ_C . Its speech universe is divided into five fuzzy sets:

- Torque error is positive large PL

- Torque error is positive small PS
- Torque error is zero ZE
- Torque error is negative small, NS
- Torque error is negative large, NL

Triangular membership functions are chosen for the sets PS, ZE and NS and trapezoidal membership functions for the sets PL and NL, Fig.8.

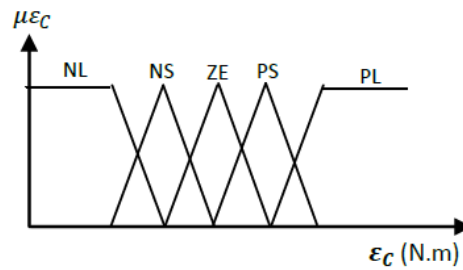


Figure 8. Membership function of torque error ϵ_C .

The third input variable is the flux position in the stator frame. The angle θ_S is given by:

$$\theta_S = \arctan \frac{\phi_{\beta S}}{\phi_{\alpha S}} \quad (14)$$

Speech universe of this variable is divided into 12 fuzzy sets (θ_1 to θ_{12}) with membership function presented in Fig.9.

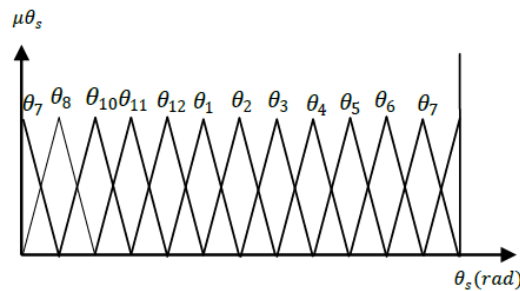


Figure 9. Position membership function.

Decomposing into six sub-outputs representing three-level inverter six switches, the speech universe of each output is divided into two fuzzy sets (zero and one) with its membership functions are chosen by forms of type presented in Fig.10 [10].

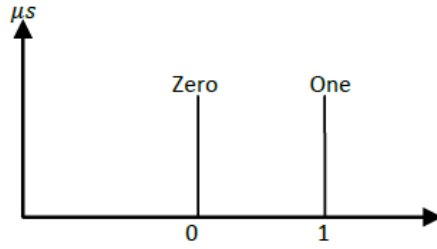


Figure 10. Membership function of switches switching states

B. Fuzzy controller structure for three-level inverter

The control rules are expressed in function of input and output variables as follows:

Ri: if ε_θ is N and ε_c is NL and θ_s is θ_1 thus, S_{11} is zero S_{12} is zero S_{21} is zero S_{22} is zero S_{31} is one S_{32} is one.

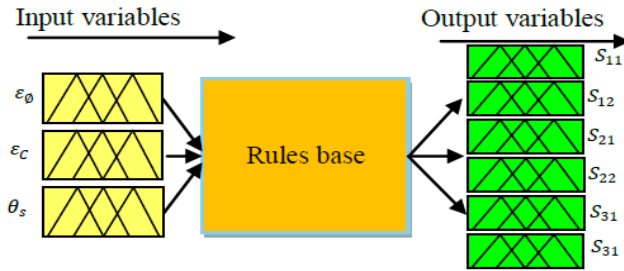


Figure 11. Fuzzy controller structure for three-level inverter.

Table 3. Switching table.

| | | | | | | | | | | | |
|------------|----|----|----|----|----|------------|----|----|----|----|----|
| θ_1 | NL | NS | ZE | PS | PL | θ_2 | NL | NS | ZE | PS | PL |
| P | 17 | 18 | 0 | 3 | 5 | P | 2 | 18 | 0 | 6 | 5 |
| Z | 13 | 0 | 0 | 4 | 4 | Z | 16 | 0 | 0 | 7 | 4 |
| N | 14 | 15 | 0 | 6 | 8 | N | 17 | 15 | 0 | 9 | 8 |
| θ_3 | NL | NS | ZE | PS | PL | θ_4 | NL | NS | ZE | PS | PL |
| P | 2 | 3 | 0 | 6 | 8 | Z | 5 | 3 | 0 | 9 | 8 |
| Z | 16 | 0 | 0 | 7 | 7 | N | 1 | 0 | 0 | 10 | 7 |
| N | 17 | 18 | 0 | 9 | 11 | P | 2 | 18 | 0 | 12 | 11 |
| θ_5 | NL | NS | ZE | PS | PL | θ_6 | NL | NS | ZE | PS | PL |
| P | 5 | 6 | 0 | 9 | 11 | P | 8 | 6 | 0 | 12 | 11 |

| | | | | | | | | | | | |
|---------------|----|----|----|----|----|---------------|----|----|----|----|----|
| Z | 1 | 0 | 0 | 10 | 10 | Z | 4 | 0 | 0 | 13 | 10 |
| N | 2 | 3 | 0 | 12 | 14 | N | 5 | 3 | 0 | 15 | 14 |
| θ_7 | NL | NS | ZE | PS | PL | θ_8 | NL | NS | ZE | PS | PL |
| P | 14 | 15 | 0 | 18 | 2 | P | 11 | 9 | 0 | 15 | 14 |
| Z | 10 | 0 | 0 | 1 | 1 | Z | 7 | 0 | 0 | 16 | 13 |
| N | 11 | 12 | 0 | 3 | 5 | N | 8 | 6 | 0 | 18 | 17 |
| θ_9 | NL | NS | ZE | PS | PL | θ_{10} | NL | NS | ZE | PS | PL |
| P | 8 | 9 | 0 | 12 | 14 | P | 14 | 12 | 0 | 18 | 17 |
| Z | 4 | 0 | 0 | 13 | 13 | Z | 10 | 0 | 0 | 1 | 16 |
| N | 5 | 6 | 0 | 15 | 17 | N | 11 | 9 | 0 | 3 | 2 |
| θ_{11} | NL | NS | ZE | PS | PL | θ_{12} | NL | NS | ZE | PS | PL |
| P | 11 | 12 | 0 | 15 | 17 | P | 17 | 15 | 0 | 3 | 2 |
| Z | 7 | 0 | 0 | 16 | 16 | Z | 13 | 0 | 0 | 4 | 1 |
| N | 8 | 9 | 0 | 18 | 2 | N | 14 | 12 | 0 | 6 | 5 |

5. Adaptive estimation of speed with reference model (MRAS)

The estimation principle using this method is based on the comparison of values obtained by two different ways, a computation which does not depend on the speed (reference model) and a computation that depends on speed (adjustable model). This method is developed by Schauder, known as Model Reference Adaptive System (MRAS) [14].

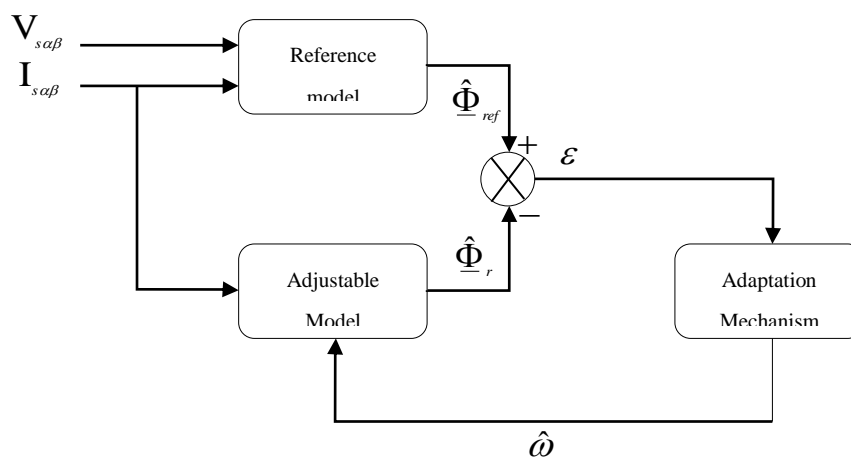


Figure 12. Estimation of asynchronous machine speed by MRAS technique.

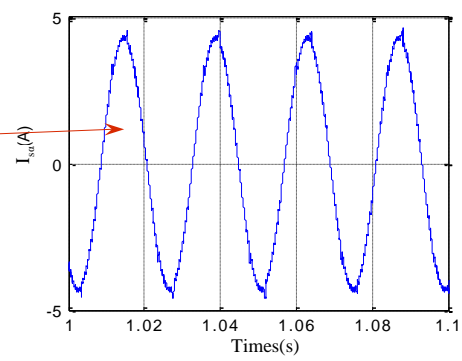
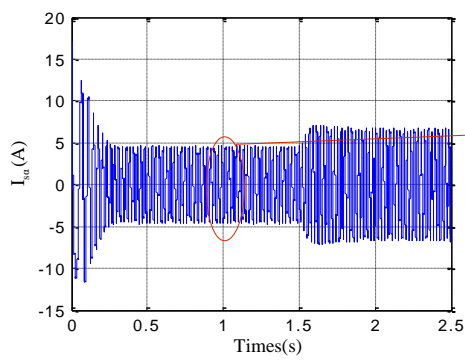
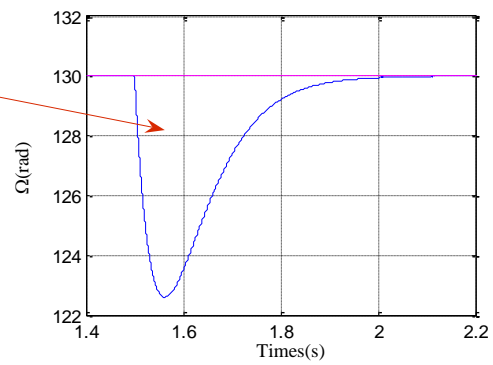
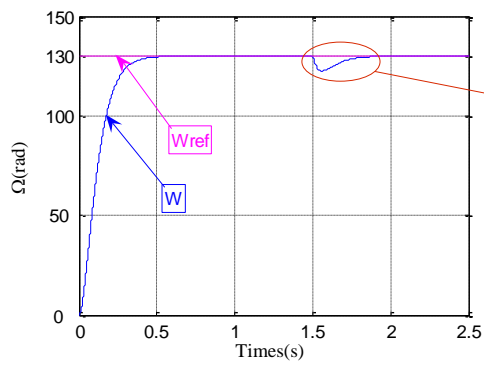
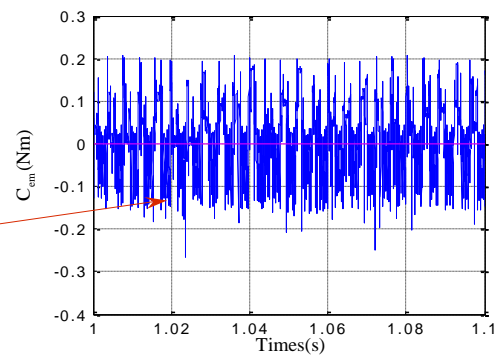
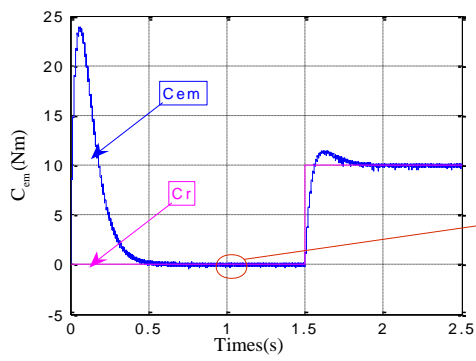
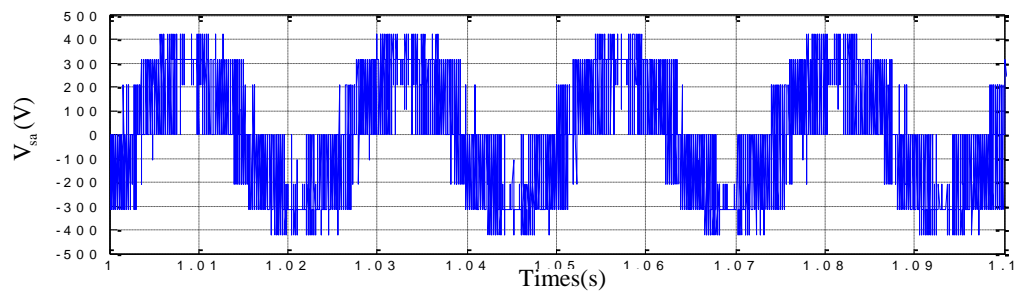
6. Simulation and results

Simulation tests were conducted using the parameters illustrated in table 4. The results shown in Fig.13 (a) and 13 (b) represent the behavior of DTC structure applied to 1.5 kW asynchronous motor fed by three-level inverter for a switching table of five-level torque corrector and three-level flux corrector in the classical and fuzzy case. Several operation characteristics were studied, such as the starting response, steady-state response and some internal variables, such as line current and voltage, stator flux, torque and speed, were viewed using Matlab simulink Blocks.

Table 4. Switching table.

| Parameters | Values |
|-----------------------------|---------------------------------|
| Voltage rating | 220 / 380 (V) |
| Current rating | 6.4 / 3.7 (A) |
| Motor power | 1.5 (kW) |
| Number of pole pairs | $p = 2$ |
| Stator resistance per phase | $R_s = 4.85 (\Omega)$ |
| Rotor resistance per phase | $R_r = 3.805 (\Omega)$ |
| Stator inductance | $L_s = 0.274 (H)$ |
| Rotor inductance | $L_r = 0.274 (H)$ |
| Mutual inductance | $L_m = 0.258 (H)$ |
| Moment of inertia | $J = 0.031 (Kg_m^2)$ |
| Speed rating | $N = 1420 (tr / min)$ |
| Friction Coefficient | $f_r = 0.000114 (Kg_m^2 / sec)$ |
| Inverter dc voltage | $U_{dc} = 514 (V)$ |
| Torque rating | $C = 10 Nm$ |

A. Classical DTC applied to asynchronous machine fed by two-level inverter



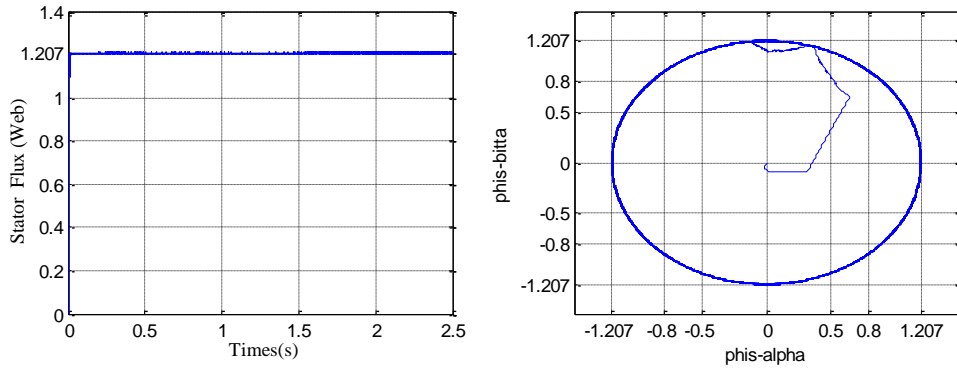
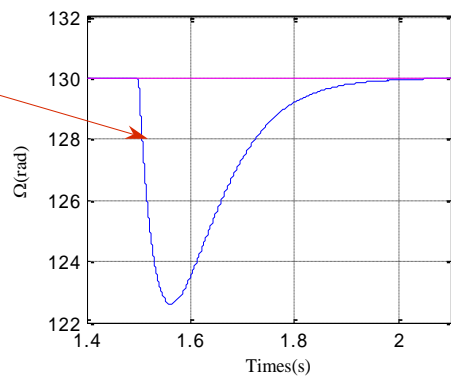
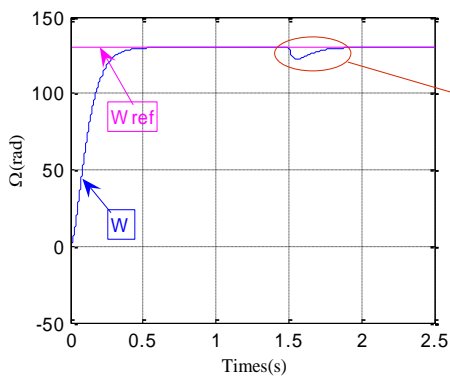
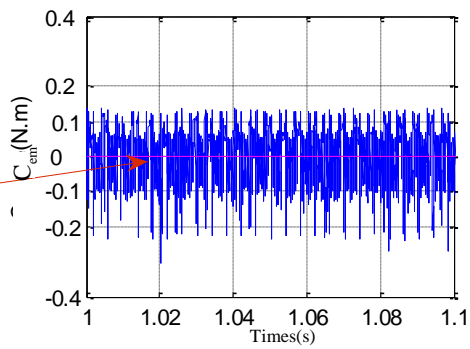
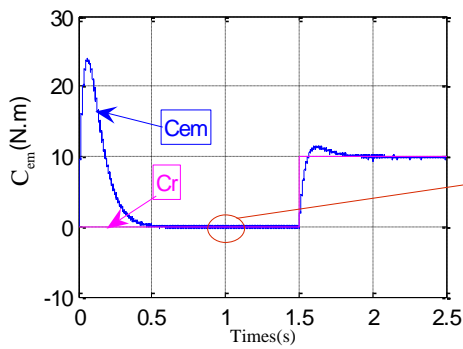
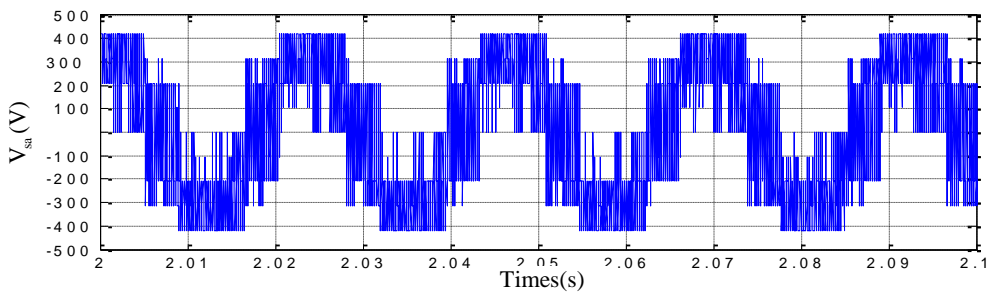


Figure 13(a). Waveforms obtained by classical DTC: phase to neutral voltages, torque, speed, current, stator flux.

B. DTC-Fuzzy technique applied to asynchronous machine fed by three-level inverter



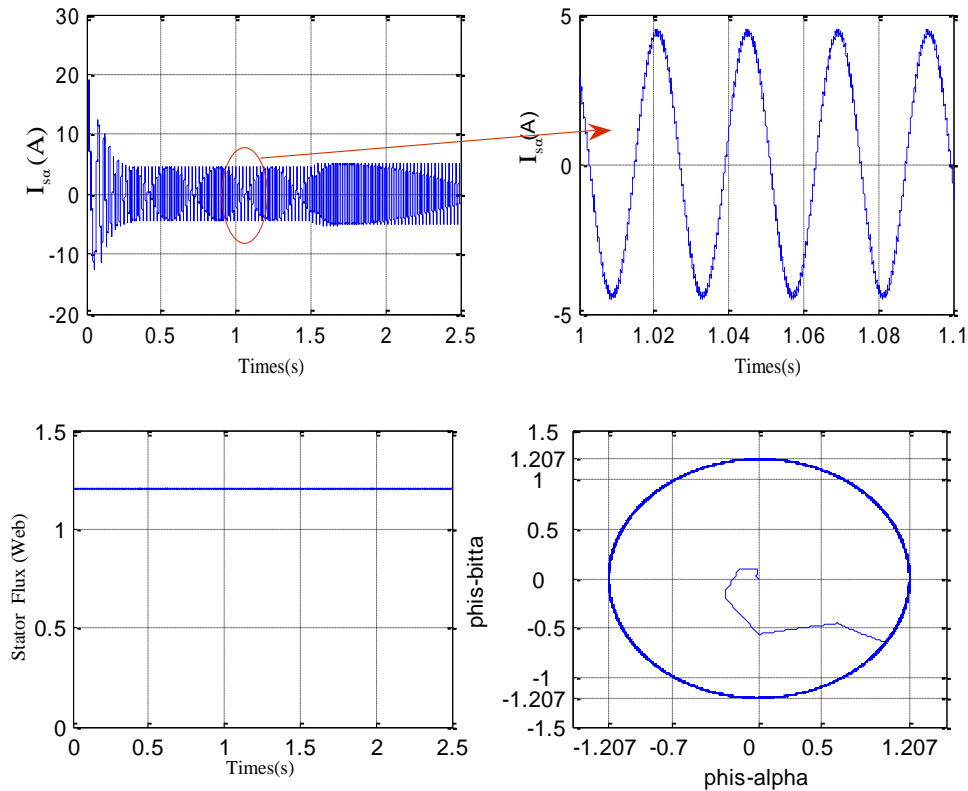


Figure 13(b). Waveforms obtained by DTC-Fuzzy technique: phase to neutral voltages, torque, speed, current, stator flux

The results have showed that in the classical DTC the speed tracks its reference without static error and the speed disturbances are minimized. The torque and flux fluctuations are reduced when DTC-fuzzy technique is used. The employment of DTC-fuzzy technique with three-level voltage inverter has improved performances compared to classical DTC with two or three-level inverters (less torque fluctuations). DTC-Fuzzy technique, presents through its fuzzy sets and inference rules a high precision in the choice of voltage vector (ensuring high switches switching). The torque in DTC-Fuzzy case presents less fluctuation compared to classical DTC fed by two-level as illustrated in Fig.13(a) and Fig.13 (b) and three-level inverter while the stator flux trajectory Φ_s has a clear and thin circular form compared to that obtained by classical DTC.

7. Conclusion

The present work has showed that the advantages of classical DTC are preserved and enhanced. The speed tracks its reference without static error and also the speed disturbance rejection is very fast. The torque and flux fluctuations are reduced especially when DTC-fuzzy technique is used, resulting in harmonics minimization and less motor problems (overheating,

vibration, ageing).

DTC-fuzzy technique associated with three-level voltage inverter has good performance compared to classical DTC with two or three-level inverters (less torque fluctuations). DTC-Fuzzy technique, presents through its fuzzy sets and inference rules a high precision in the choice of voltage vector (ensuring high switches switching).

References

1. Talaeizadeh V., Kianinezhad R., Seyfossadat S., Shayanfar H, Direct Torque Control of Six-phase Induction Motors Using Three-phase Matrix Converter, 2010, Energy Conversion and Management, vol. 51, pp. 2482-2491.
2. A. Khedher, M.-F. Mimouni, Sensorless-adaptive DTC of double star induction motor, 2010, Energy Conversion and Management, vol. 51, pp. 2878–2892.
3. E. Benyoussef, A. Meroufel, S. Barkat, Three-Level Direct Torque Control Based on Artificial Neural Network of Double Star Synchronous Machine, Leonardo Journal of Sciences, no. 24, January-June 2014, p. 15-27.
4. Giuseppe S. Buja, Marian P. Kazmierkowski, Direct Torque Control for Induction Motor with broken bars using Fuzzy Logic Type-2, AMSE Journals –2015-Series: Modelling C, vol. 70, no. 1, pp. 15-28.
5. A. Arif, A. Betka, A. Guettaf, Modelling and simulation on direct torque control (DTC) system for electric vehicle (EV) induction motors. AMSE JOURNALS–2011-Series: Modelling C, vol. 68, no. 2, pp. 29-41.
6. Yongchang Zhang, Jianguo Zhu, Zhengming Zhao, Wei Xu, David G. Dorrell, An Improved Direct Torque Control for Three-Level Inverter-Fed Induction Motor Sensorless Drive, March 2012, IEEE Transactions on Industrial electronics, vol. 27, no. 3, pp. 1502-1512.
7. B. Singh, N. Mittal, D. Verma, D. Singh, S. Singh, R. Dixit, M. Singh, A. Baranwal, Multi-Level Inverter: A Literature Survey on Topologies and Control Strategies, 2012, International Journal of Reviews in Computing, vol. 10, pp. 1-16.

8. H. Hosni, A. Hmidet, O. Hasnaoui, DTC-SVM control for three phase induction motors, International Conference on Electrical Engineering and Software Applications (ICEESA), 2013.
9. K. S. Manoj, K. P. Anup, P. P. Bibhu, Direct Torque Control for Three-Level Neutral Point Clamped Inverter-Fed Induction Motor Drive, 2012, ETASR - Engineering, Technology & Applied Science Research, vol. 2, no. 2, pp. 201-208.
10. Y. Gao, J. Wang, X. Qiu, The Improvement of DTC System Performance on Fuzzy Control, Procedia Environmental Sciences, 2011, vol. 10, pp. 589-594.
11. L. Benalia, A. Chaghi, R. Abdessemed, A Robust DTC Applied to the Doubly Stator Asynchronous Motor Based on RST Regulator, 2013, Journal of Electrical and Control Engineering vol. 3, no. 3, pp. 25-30.
12. R. Kennel, E.E. El-kholy, S. Mahmoud, A. El-refaei, F. Elkady, Improved direct torque control for induction motor drives with rapid prototyping system, Energy Convers Manage 2006, vol. 46, pp. 1999–2010.
13. R. Abdelli, D. Rekioua, T. Rekioua, A. Tounsi, Improved direct torque control of an induction generator used in a wind conversion system connected to the grid, 2013, ISA Transactions, vol. 52, pp. 525–538.
14. M. Comanescu, L. Xu. Sliding-mode MRAS speed estimators for sensorless vector control of induction machine, 2006, IEEE Trans Ind. Electron, vol. 53, no. 1, pp. 146–53.
15. S. Saad, L. Zellouma, Fuzzy logic controller for three-level shunt active filter compensating harmonics and reactive power, 2009, Electric Power Systems Research, vol. 79, pp. 1337–1341.